

# Characterizing Aerosol Lidar Ratio Variations for Possible Improvement in Extinction Retrievals

Jay Kar<sup>1,2</sup>, Chip Trepte<sup>2</sup>, Mark Vaughan<sup>2</sup>, Jason Tackett<sup>2</sup>,  
Greg Schuster<sup>2</sup>, Pat Lucker<sup>1,2</sup>

<sup>1</sup> Science Systems and Applications, Inc. (SSAI)

<sup>2</sup> NASA Langley Research Center

The equation for elastic-backscatter lidar needs to solve for 2 unknowns ( $\beta_p$  and  $\sigma_p$ ) from 1 equation:

$$\beta_p(r) = (\beta'(r) / T_m^2 T_{O_3}^2 T_p^2) - \beta_m(r) \quad (1)$$

Known from atmospheric models

$$T_p^2(r) = \exp \left[ -2 \eta(r) \int_{r_0}^r \sigma_p(r') dr', \right] \quad (2)$$

Assume a lidar ratio  $S = \sigma_p(r) / \beta_p(r)$  and solve the equation

- Mostly lidar ratios are taken from a look-up table ---best estimates from various sources
- A spatially and vertically constant value is used for various types of aerosol (smoke, dust..)
- This methodology is used for spaceborne lidars like CALIPSO, CATS
- Over the years, significant variability of lidar ratio has been observed for various species
- We shall attempt to provide a glimpse of this variability from various available sources.



# Different Methods of Estimating Lidar Ratios



- Raman Lidars -- Independent retrievals of extinction and backscatter  
-- Estimated uncertainties of  $\sim 10\text{-}20\%$   
-- Very low SNR during daytime
- HSRL -- Independent retrievals of extinction and backscatter  
-- Estimated uncertainty  $\sim 9\%$  for typical AOD of 0.2
- Elastic backscatter -- Constrained by AOD from photometer, satellites (e.g. MODIS)  
-- Column averaged estimate of lidar ratio  
-- Estimated uncertainty of  $\sim 10\text{-}30\%$
- AERONET -- Lidar ratio retrieved from phase function and SSA  
-- Uses size distribution and refractive indices  
-- Estimated uncertainties of 8-15% depending upon site and wavelength
- Spaceborne -- SODA (using CloudSat/CALIOP data), POLDER
- Models -- Mie calculations, T matrix calculations



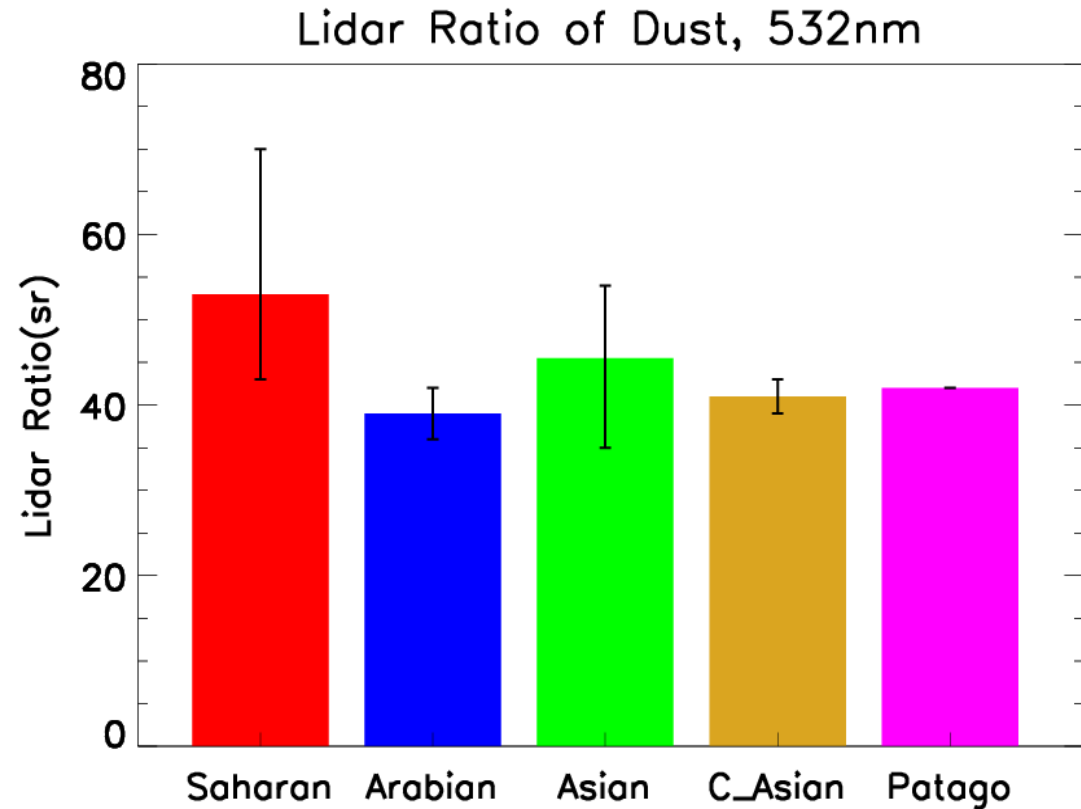
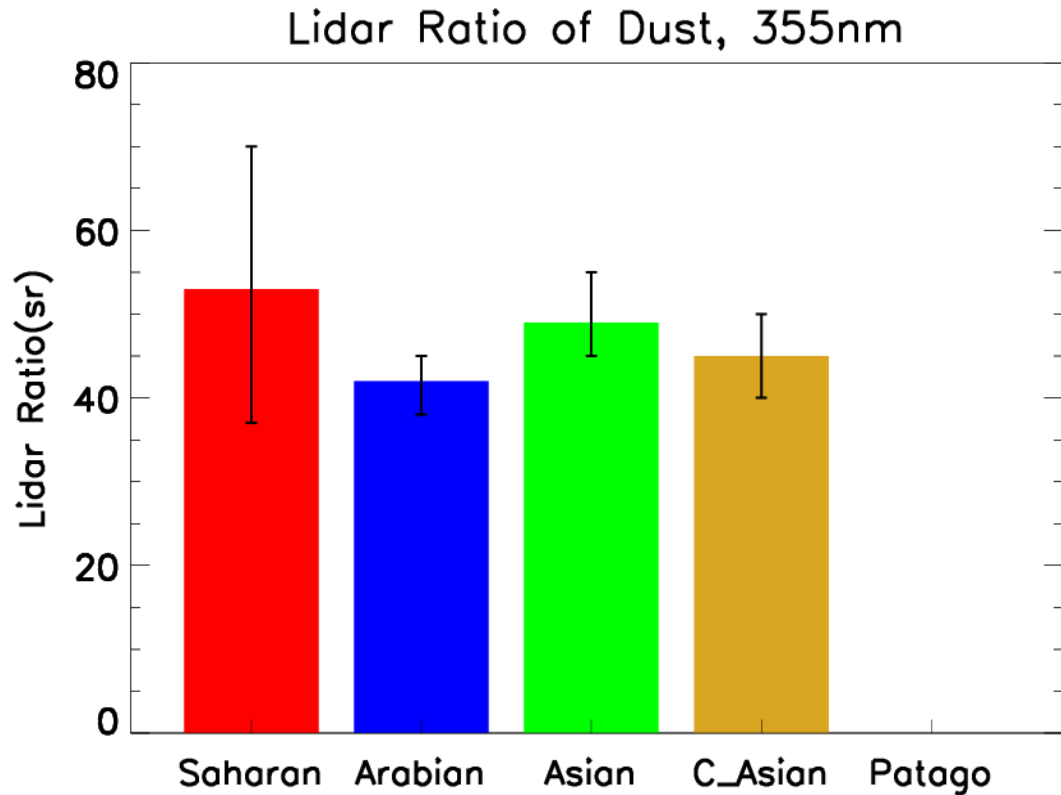
- European Aerosol Research Lidar Network (EARLINET/ACTRIX) (Pappalardo et al., 2014)
  - 30 stations, 16 countries, mostly Raman lidars, lidar ratio at 355 nm, 532 nm
- Asian Dust and Aerosol Lidar Network (ADNET) (Nishizawa et al., 2017)
  - ~ 20 sites in East Asia some with Raman channels, 355 nm, 532 nm
- Latin American Lidar Network (LALINET) (Antuna-Marrero et al., 2017)
  - 14 stations operating currently, some Raman, most with AERONET sun photometers, 532 nm
- Pollynet (Baars et al., 2016)
  - Network of portable remote-controlled Raman lidars
  - Deployed in > 20 locations in Europe including high latitudes (Finland), Polarstern cruises, Amazon rain forest, several countries in Asia, South Africa, and Chile, 355 nm and 532 nm
- Micro-Pulse Lidar Network (MPLNET) (Welton et al., 2018)
  - Over 70 sites, 20 active, elastic backscatter, 532 nm



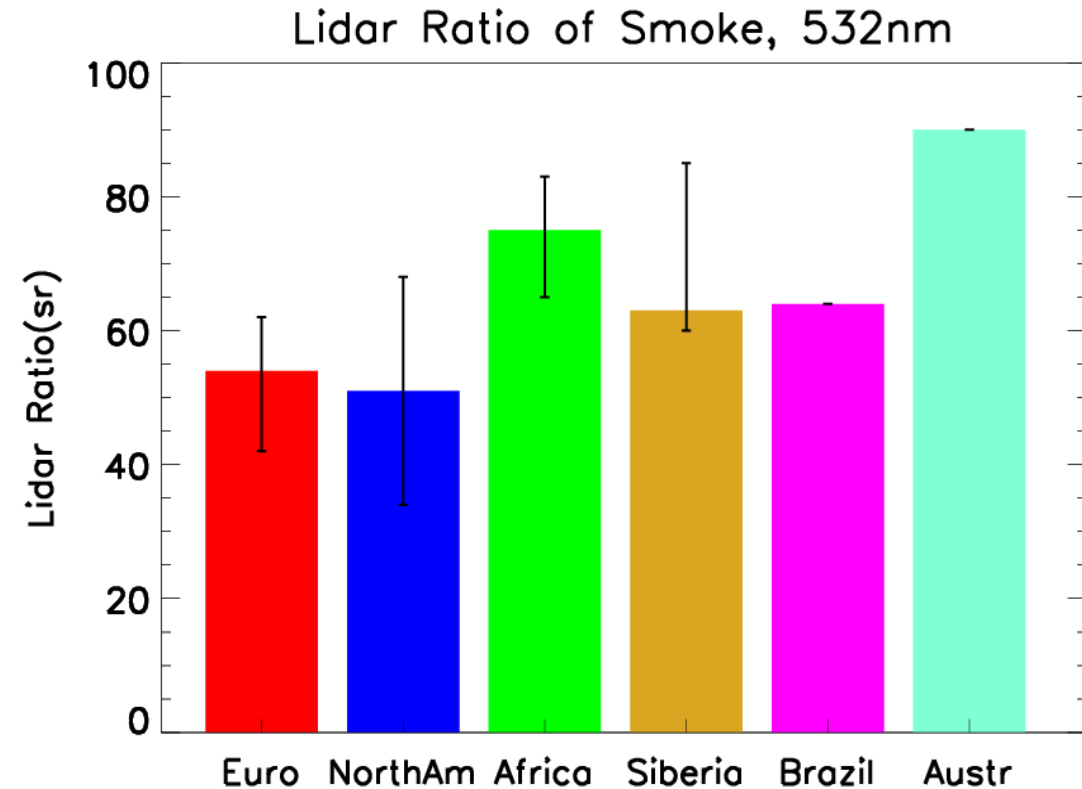
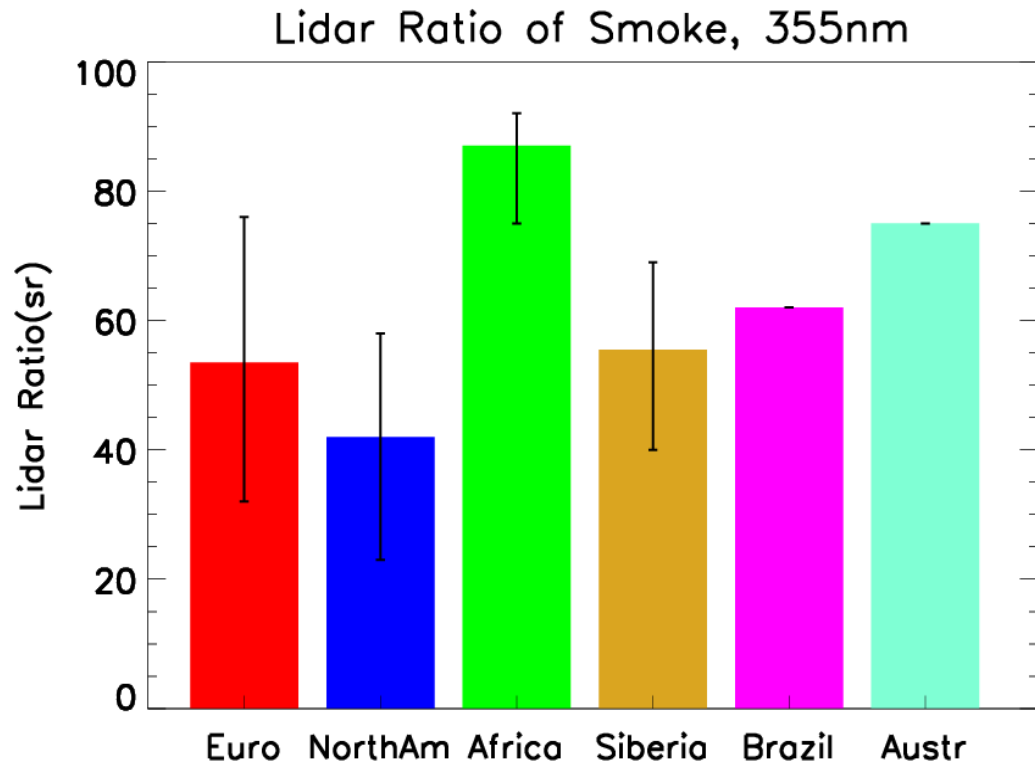
- NASA Langley airborne HSRL
  - HSRL1 → 19 field campaigns over North America between 2006-2012, 532 nm (Hair et al., 2008, Burton et al. 2012)
  - HSRL2 → Uses HSRL technique at both 355 nm and 532 nm, deployed in ORACLES (Burton et al. 2018)
- DLR airborne HSRL campaigns over Europe, Africa, Cape Verde islands, 532 nm, (SAMUM1, SAMUM2) (Groß et al., 2013)
- Shipborne trans-Atlantic and Arctic campaigns, 355 nm, 532 nm (Kanitz et al., 2013, 2014, Engelmann et al., 2020)
- Ground based mobile campaign from Paris to lake Baikal in Russia, 355 nm (Dieudonne et al., 2015)



- Climatologies available from different measurement networks
- Climatologies available from models
- Regional variations
- Diurnal variations
- Seasonal variations
- Variations with Relative Humidity
- Variations with Age of particles
- Mixing

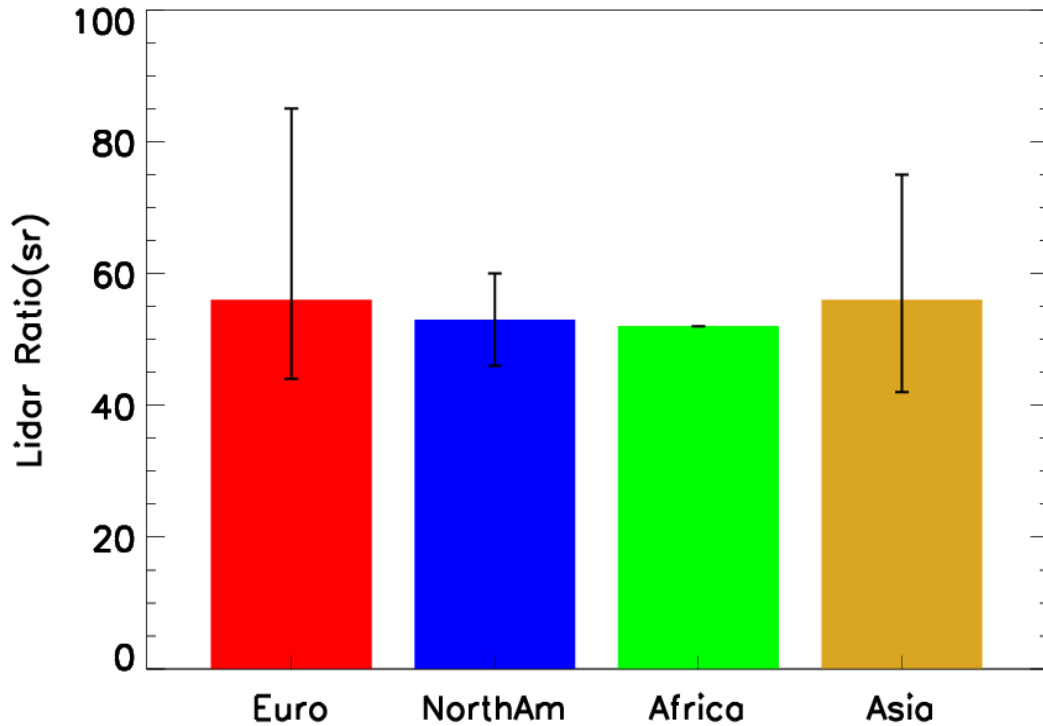


- Retrieved lidar ratios from Raman lidars and HSRL only are used (from publications)
- Bars represent medians and the error bars indicate the range of values
- Lidar ratio of Saharan dust is higher than others
- Only measurement of Patagonian dust available at 532 nm from shipborne measurements (Kanitz et al., 2013)

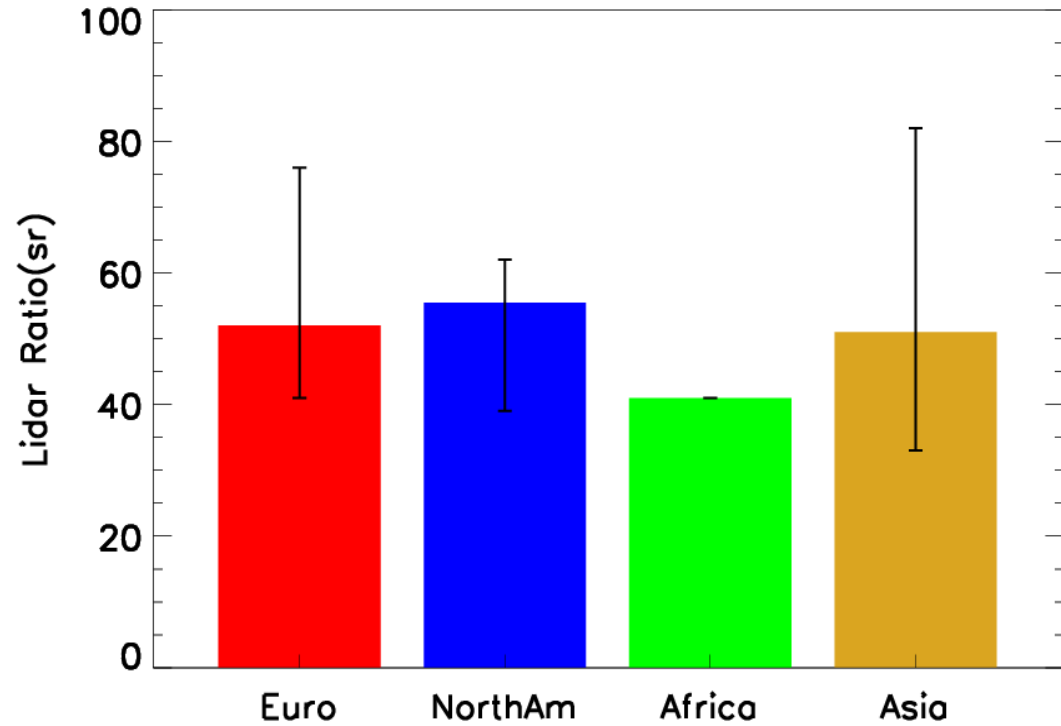


- Lidar ratio of African smoke is higher than others
- Australian smoke refers to the pyroCb events of January 2020 (Ohneiser et al., 2020)
- Lidar ratio of smoke particles changes with age and depends on wavelength with ratio of the lidar ratios at 532 nm to 355 nm changing from  $< 1$  for fresh smoke to  $> 1$  for aged smoke (Muller et al., 2007, Nicolae et al. 2013, Burton et al., 2018)

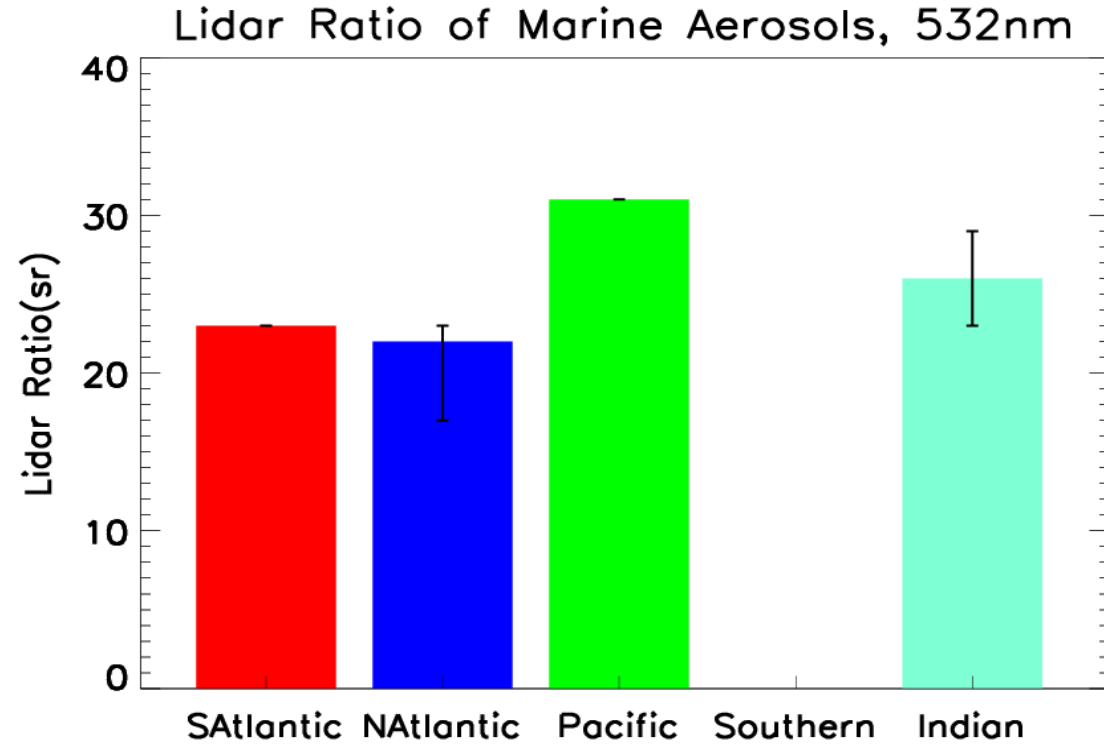
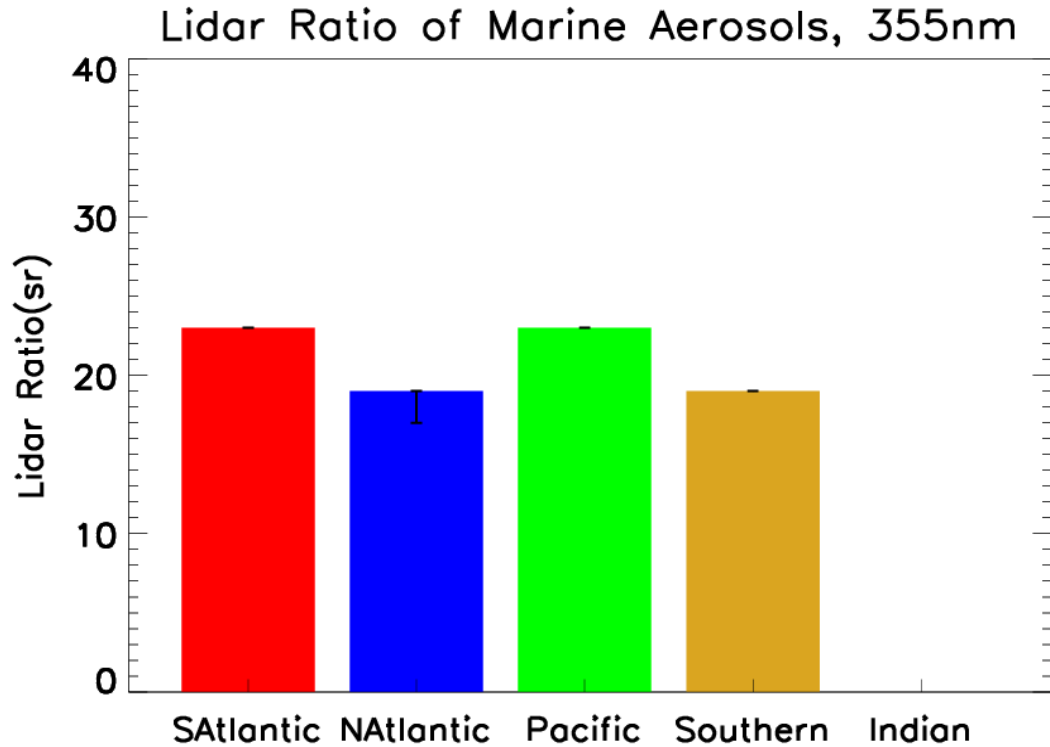
Lidar Ratio of Pollution, 355nm



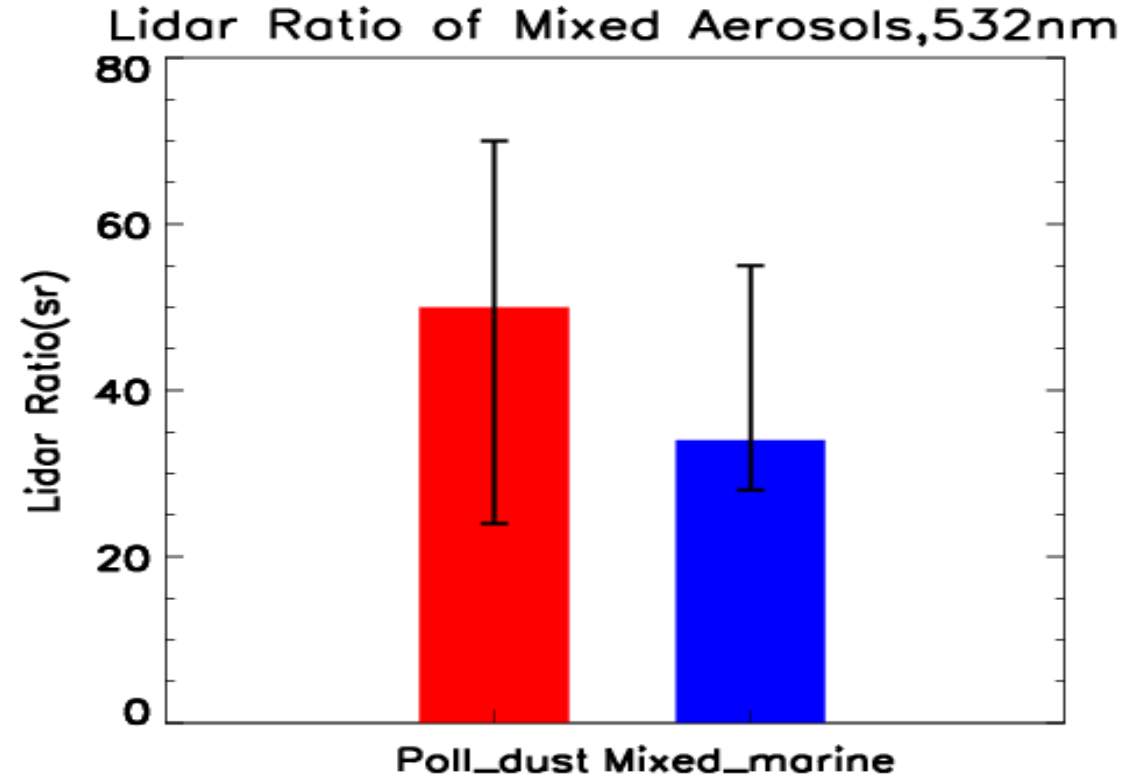
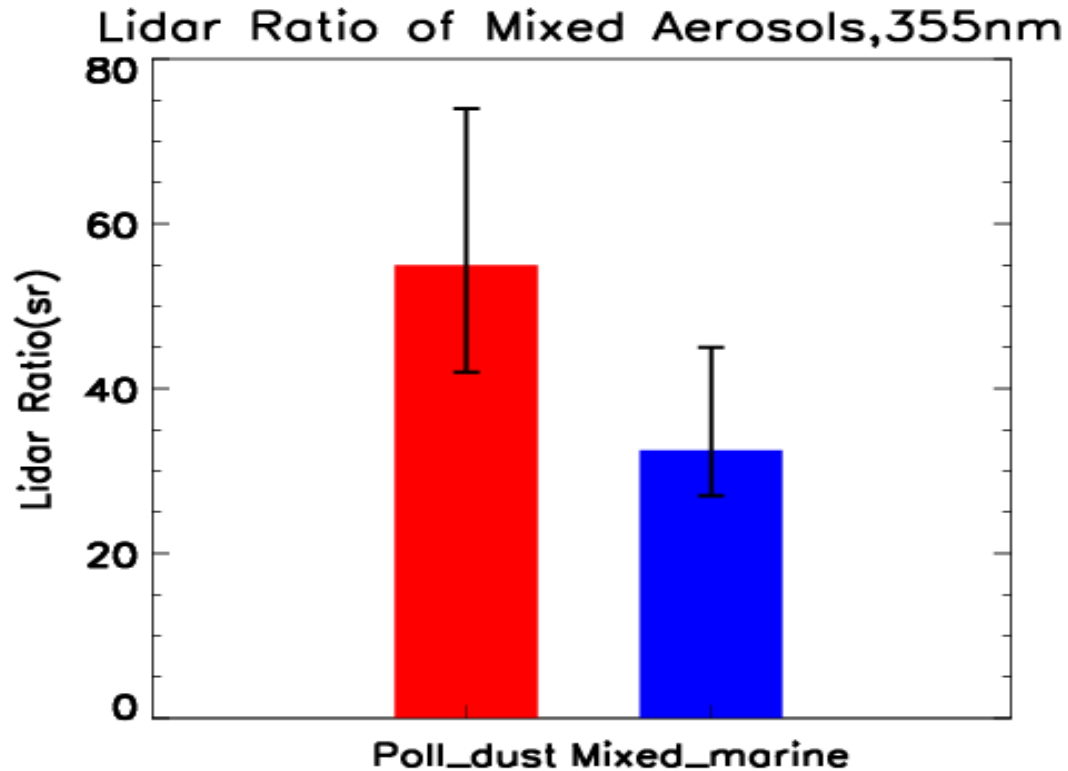
Lidar Ratio of Pollution, 532nm



- Lidar ratios of pollution including urban haze, polluted continental and industrial aerosols
- Low SNR of Raman lidars during daytime poses problems for characterizing diurnal variations of lidar ratios. Significant diurnal variation of lidar ratio over Paris (at 355 nm) was observed during strong winter pollution events (Baron et al., 2020)



- Lidar ratios of marine aerosols are lowest among all species.



- Characterizing lidar ratios of mixtures of aerosols is challenging
- Polluted dust is mixture of pollution or smoke with dust
- Mixed marine is mixture of marine and dust or other aerosol

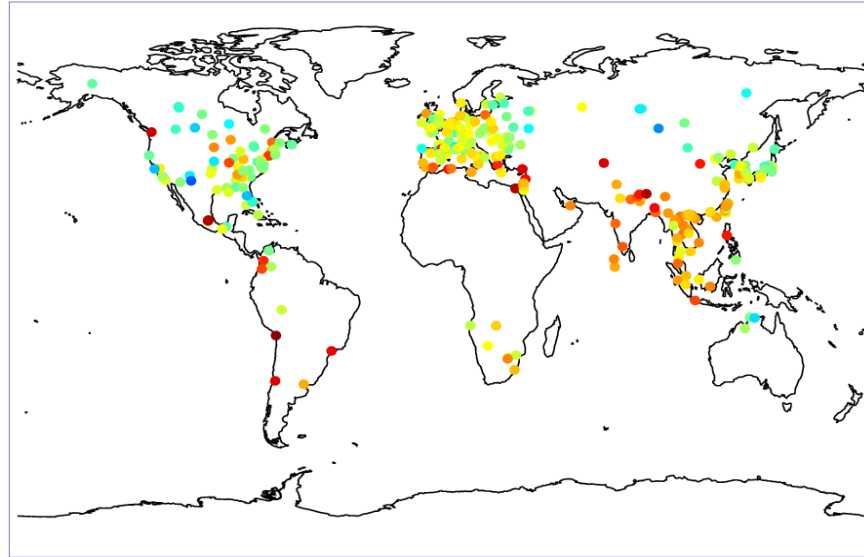
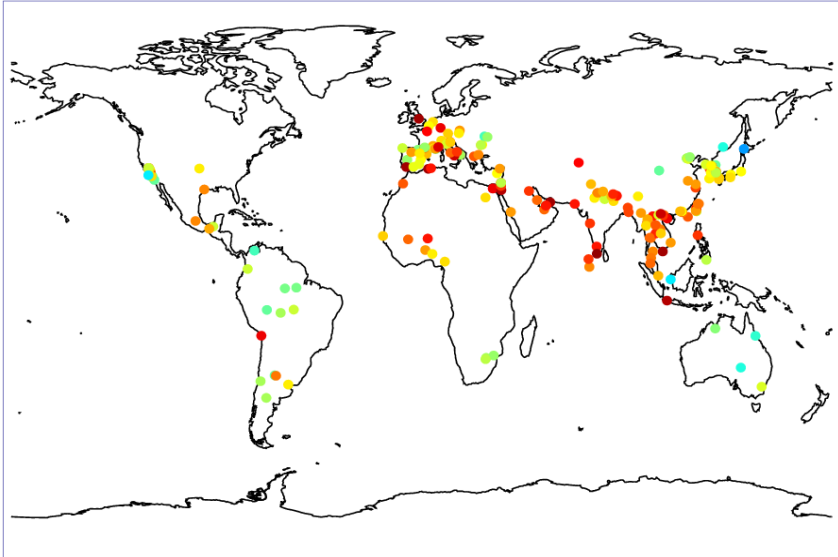


- AERONET is a global ground based network of radiometers (~ 500)
- Measure direct solar intensity and sky radiance at several solar azimuth angles
- AOD, size distribution and other parameters are retrieved from these measurements—lidar ratio retrieved from SSA and phase matrix
- Version 3 AERONET product provides the lidar ratio at 440 nm, 675 nm, 870 nm and 1020 nm.
- Lidar ratio at 532 nm interpolated from 440 nm and 675 nm
- Fine volume fraction (fvf) is used to study the variation of lidar ratios,  $fvf < 0.1$  for coarse mode and  $fvf > 0.5$  for fine mode.

**DJF**

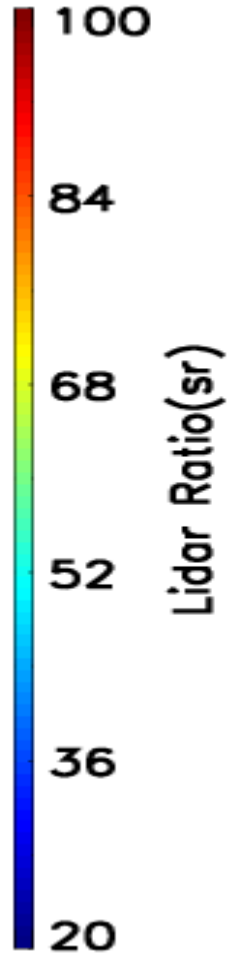
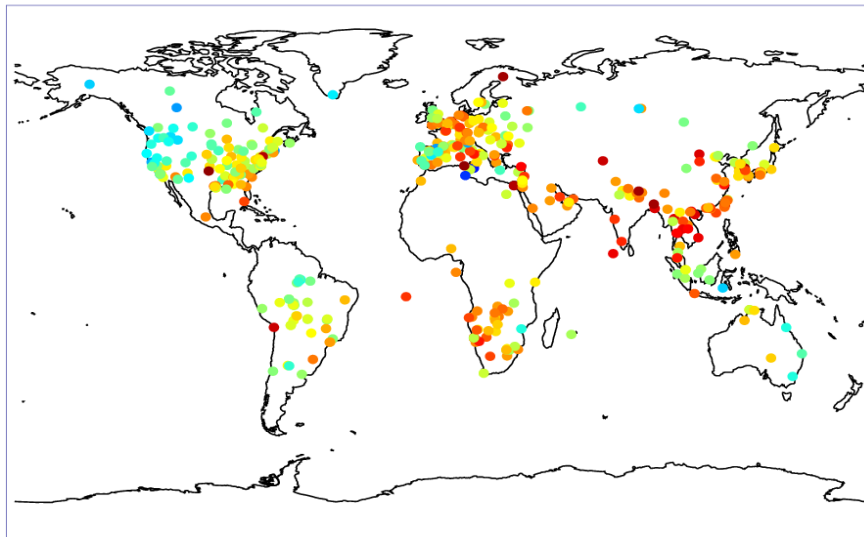
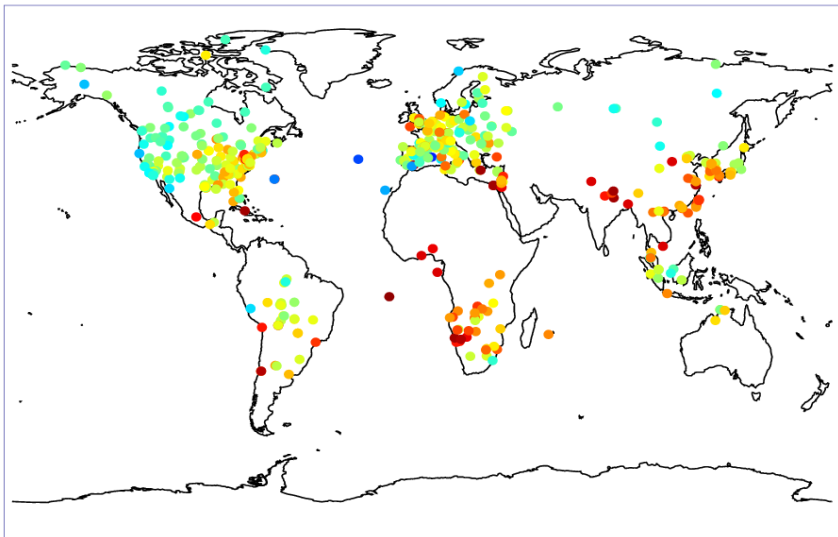
**Fine (fvf > 0.5)**

**MAM**



**JJA**

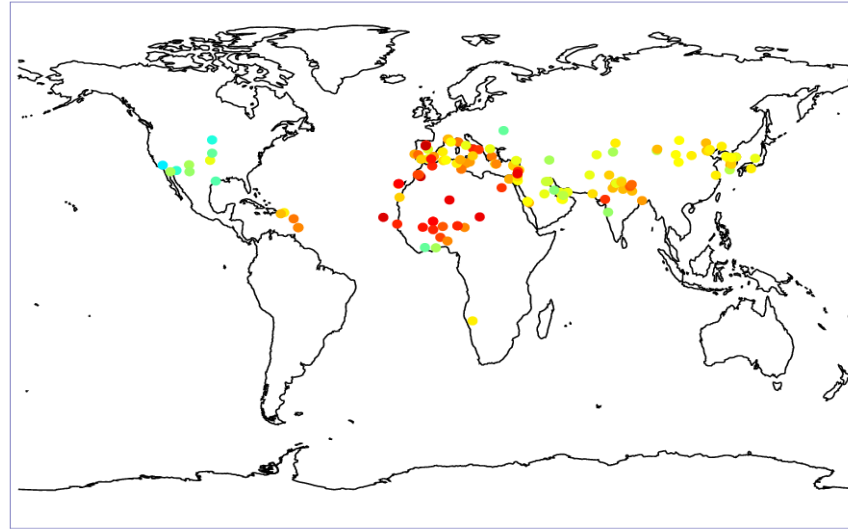
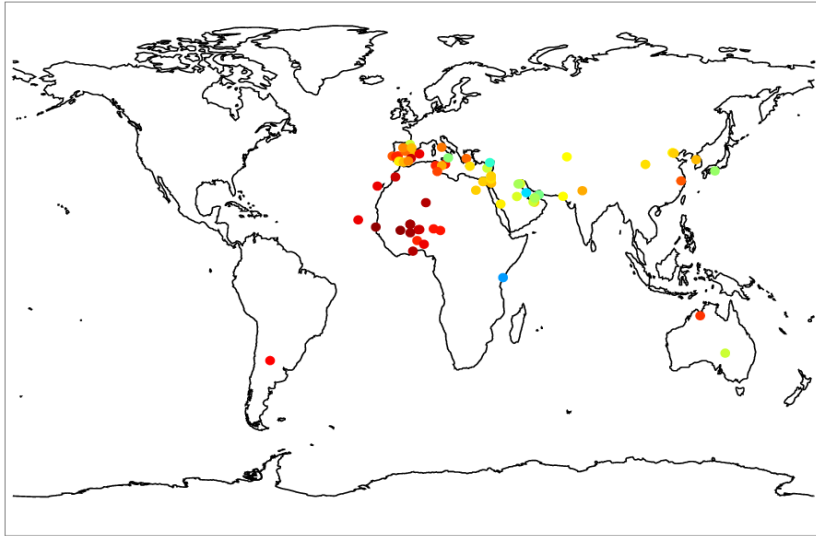
**SON**



**DJF**

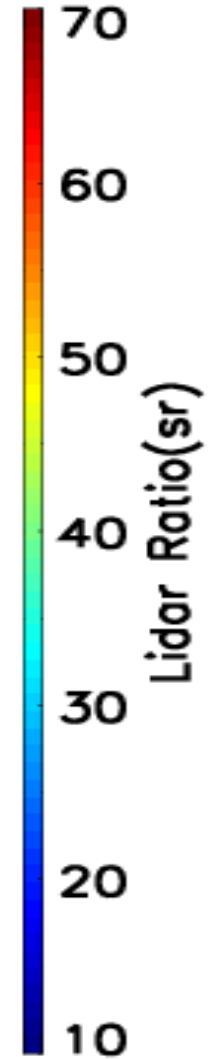
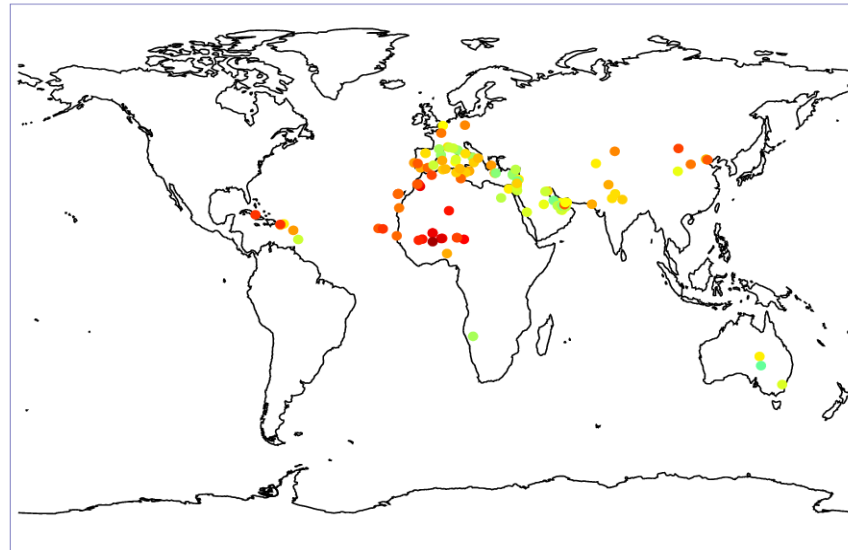
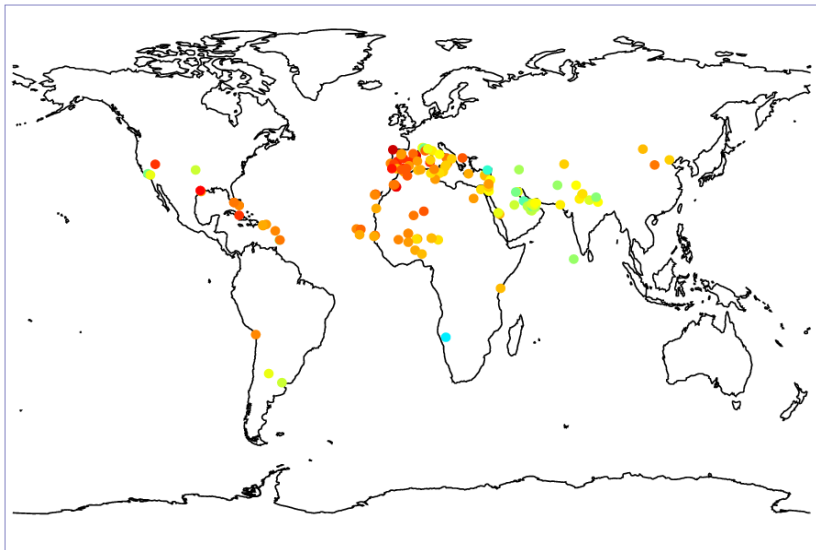
**Coarse (fvf < 0.1)**

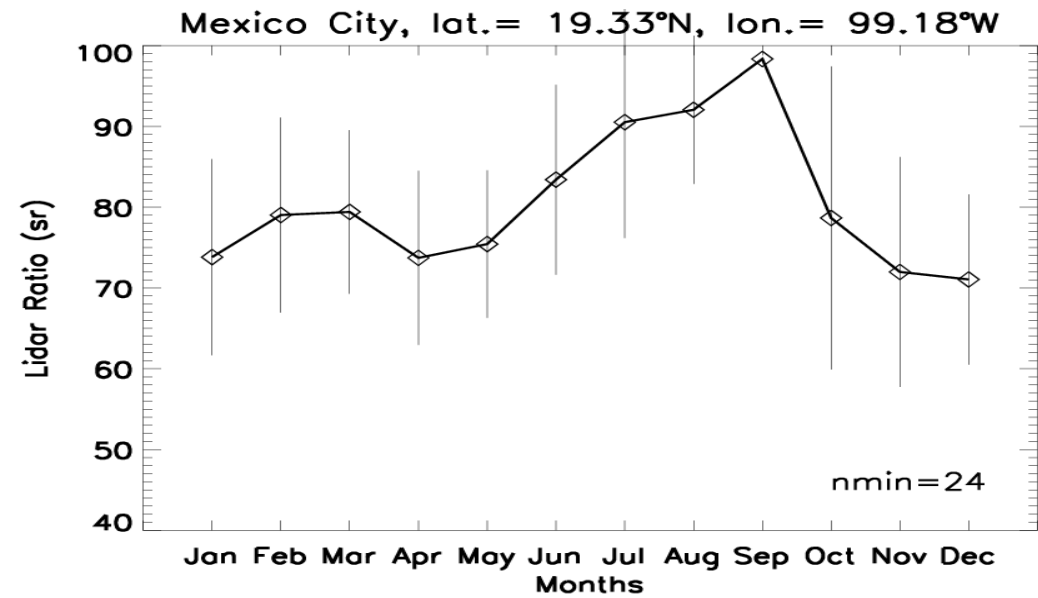
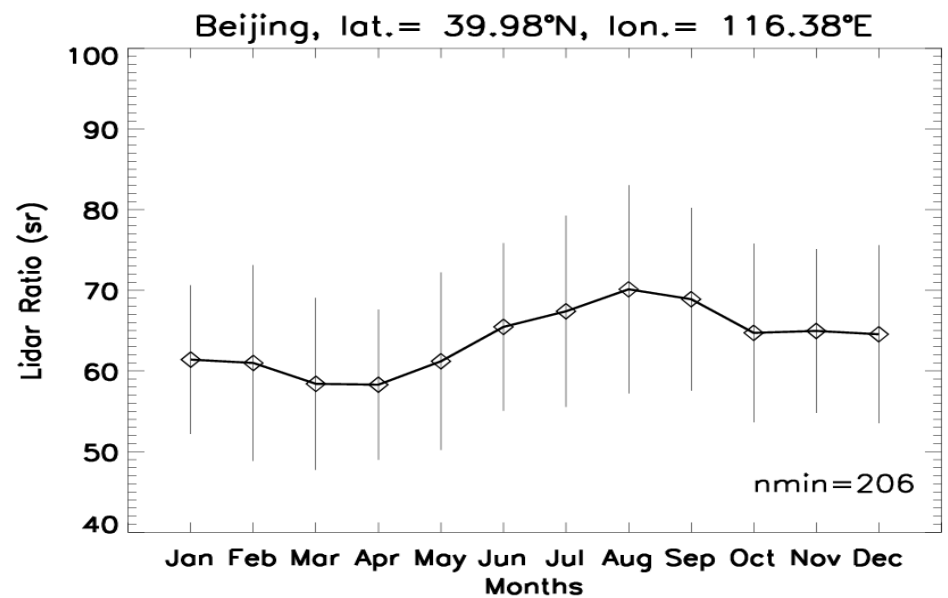
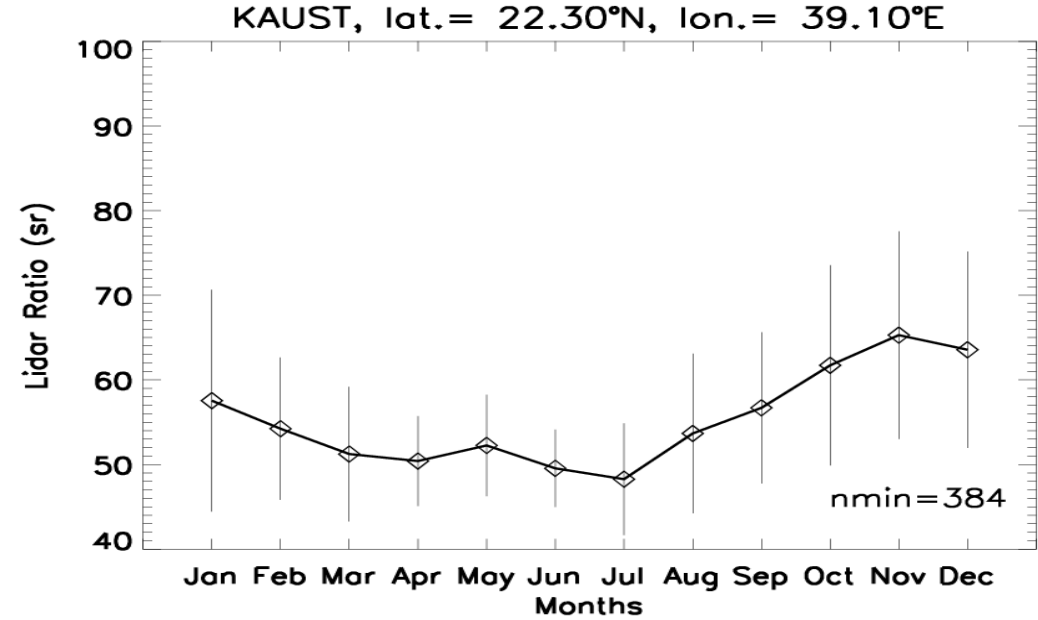
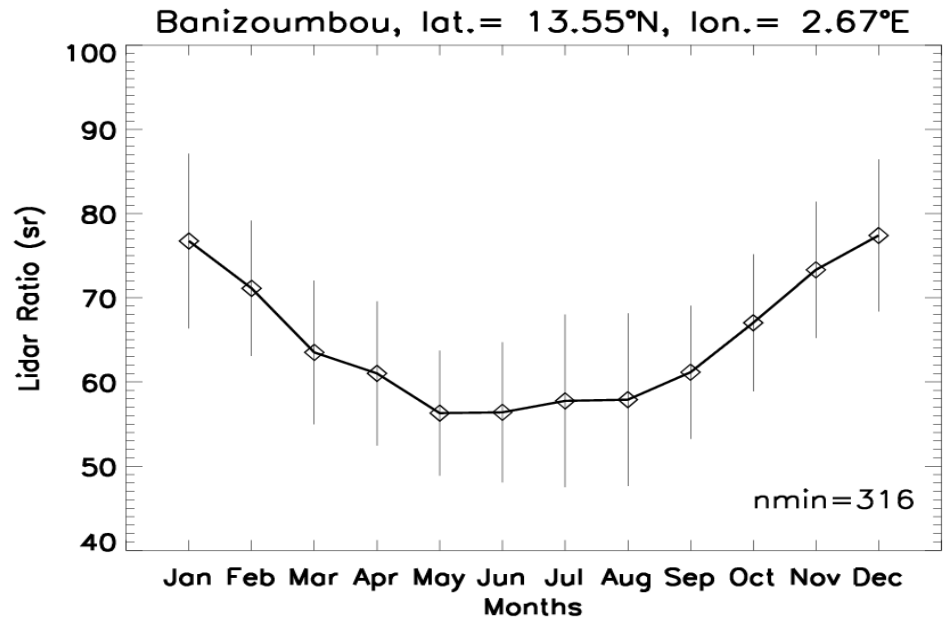
**MAM**



**JJA**

**SON**







- Lidar ratios vary significantly regionally and seasonally.
- Current and future lidar missions will need to incorporate these variations in order to provide reliable aerosol loading estimates.
- Sparse data over several areas including Australia and South America.

- Antuna-Marrero, J. C. et al., doi:10.1175/BAMS-D-15-0028.1, 2017.
- Baars, H. et al., ACP, 16, 5111–5137, 2016.
- Baron, A., ACP, <https://doi.org/10.5194/acp-20-6749-2020>, 2020.
- Burton, S. P. et al., AMT, 5, 73-98, doi:10.5194/amt-5-73-2012, 2012.
- Burton, S. P., et al., Appl. Opt., 57, 6061-6075, <https://doi.org/10.1364/AO.57.006061>, 2018.
- Dieudonne, E. et al., ACP, 15, 5007-5026, doi:10.5194/ACP-15-5007-2015, 2015.
- Engelmann, et al., ACPD, <https://doi.org/10.5194/acp-2020-1271>, 2020.
- Groß, S., et al., ACP, 13, 2487-2505, doi:10.5194/acp-13-2487-2013, 2013.
- Hair, J. W. et al., Appl. Optics, 47, 6734–6752, doi:10.1364/AO.47.006734, 2008.
- Kanitz, T. et al., JGR, 118, 2643–2655, doi:10.1002/jgrd.50273, 2013.
- Kanitz, T. et al., GRL, 41, 1044-1050, doi:10.1002/2013GL058780, 2014.
- MOSAIC, <https://mosaic-expedition.org/>
- Müller, D. et al., JGR, 112, D16202, doi:10.1029/2006JD008292, 2007.
- Nicolae, D. et al., JGR, 118, 2956-2965, doi:10.1002/jgrd.50324, 2013.
- Nishizawa, T., et al., <http://dx.doi.org/10.1016/j.jqsrt.2016.06.031>, 2017.
- Ohneiser, K., et al., <https://doi.org/10.5194/acp-20-8003-2020>.
- Pappalardo, G., et al., AMT, 7, 2389-2409, doi:10.5194/amt-7-2389-2014, 2014.
- Welton, E. J., et al., <https://doi.org/10.1051/epjconf/201817609003>, 2018.